

## CHAPTER 119

### Littoral Drift Model for Natural Environments

Rolf Deigaard <sup>1)</sup>, Jørgen Fredsøe <sup>2)</sup>, Ida Brøker Hedegaard <sup>1)</sup>  
Julio A. Zyberman <sup>2)</sup> and Ole Holst Andersen <sup>1)</sup>

#### ABSTRACT

The littoral drift model developed at DHI and ISVA, see Deigaard et al. (1986b) has been extended to include the effects of the irregularity of the waves, of a coastal current and a wind acting on the surf zone. Further, a mathematical model to simulate the near-shore current pattern along a barred coast with rip channels has been developed.

The influence on the littoral drift of the irregularity of waves, wind, coastal current, and rip channels is discussed. It is concluded that irregularity of waves and presence of rip channels must be considered while coastal current and wind action are of minor importance.

#### INTRODUCTION

The modelling of longshore sediment transport has been improved significantly during the last decade. From formulae based on 'longshore energy flux' originating from the incoming waves, a more detailed formulation of the problem is now appearing. However, it is common to most of the approaches that the description still relies on regular incoming waves which meet a coast with a constant slope, and with quasi-uniform longshore conditions.

The purpose of this paper is to discuss the influence on the littoral drift of the natural variability of waves and coastal profiles. Besides analysis is carried out of the effect on the littoral drift of a coastal current and a wind blowing over the surf zone.

The starting point of the present analysis is the littoral drift model, developed at DHI and ISVA, and described by Deigaard et al. (1986b). It is a mathematical model which consists of two main elements.

- 
- 1) Danish Hydraulic Institute (DHI), Agern Allé 5, DK-2970, Hørsholm, Denmark.
  - 2) Institute of Hydrodynamics and Hydraulic Eng. (ISVA), Technical University of Denmark, DK-2800 Lyngby, Denmark.

- A hydrodynamic module describing the wave height and direction in the coastal zone and the wave generated littoral current.
- A sediment transport module which calculates the local sediment transport rate as a function of the local hydraulic parameters. The sediment transport rate is integrated over the coastal profile.

The processes involved in wave transformation are refraction, shoaling and breaking. The associated variation in radiation stresses is used to calculate the shore normal component causing a wave set-up and the shear component of the radiation stress,  $S_{xy}$ . The shear component is driving the littoral current,  $\tau_b$  is constant outside the breaker line where no energy dissipation occurs. The littoral current is calculated from the balance between bed shear stress  $\tau_b$ , cross-shore momentum exchange and the gradient in shear radiation stress:

$$\tau_b - \frac{d}{dx} (\rho E D \frac{dV}{dx}) = - \frac{dS_{xy}}{dx} \quad (1)$$

where  $x$  is the cross-shore coordinate,  $\rho$  is the density of water,  $E$  the momentum exchange coefficient,  $D$  the water depth, and  $V$  is the depth averaged littoral drift velocity.

The local sediment transport is calculated by the model described by Fredsøe (1984), Fredsøe et al. (1985), and Deigaard et al. (1986a). The bed load and suspended load transport is calculated separately. The suspended load is normally dominant in the surf zone; it is described by the vertical turbulent diffusion equation:

$$\frac{\partial c}{\partial t} = \frac{\partial}{\partial z} (\epsilon_s \frac{\partial c}{\partial z}) + w \frac{\partial c}{\partial z} \quad (2)$$

where  $z$  is the vertical coordinate,  $c$  the sediment concentration,  $t$  is time,  $\epsilon_s$  turbulent diffusion coefficient, and  $w$  is the settling velocity.  $\epsilon_s$  is calculated by taking the turbulent wave-current boundary layer as well as the turbulence generated by breaking or broken waves into account. The boundary conditions for Eq. (2) are zero flux of sediment through the water surface and a time-varying near-bed concentration calculated by the model of Engelund and Fredsøe (1976).

Fig. 1 gives an example of model results showing the profile of the littoral current and the littoral sediment transport rate across a coastal profile with one longshore bar.

The above described model has a number of limitations, the most important being:

- the incoming waves are unidirectional and regular
- the conditions along the coast are uniform
- only driving forces from the waves are included.

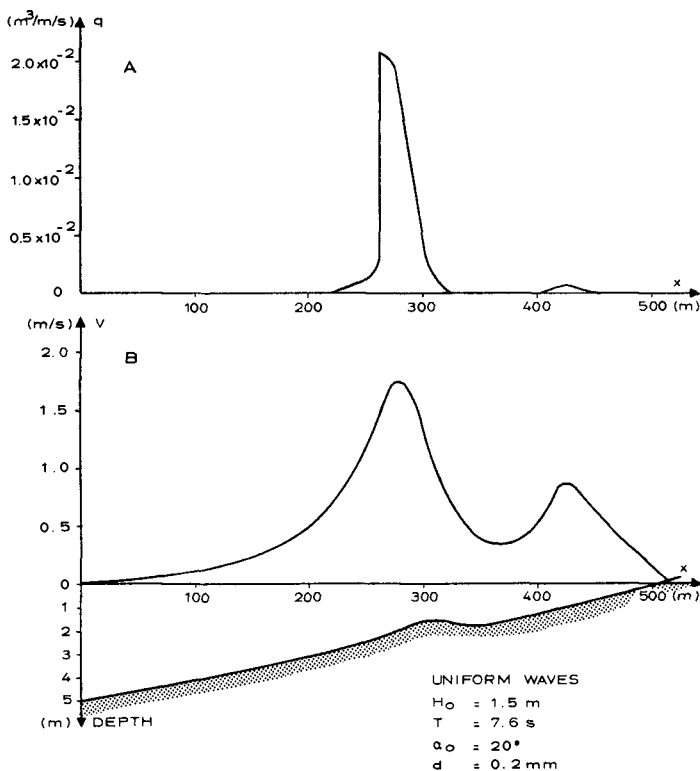


Fig. 1. Example of model results.

**A:** Littoral Sediment Transport Rates.  
**B:** Profile of Littoral Current and Coastal Profile.

In the following it is described, how the model has been modified to overcome these limitations, and the effect of the various mechanisms treated is discussed.

#### IRREGULAR WAVES

The effect of irregular waves versus regular monochromatic waves has been included in the modelling of the long-shore current as well as of the sediment transport rate.

The longshore current velocity profile driven by irregular waves with directional spreading was analysed in detail by Battjes (1974) and the present model conforms with his results. The present model describes the irregular wave situation as a series of regular wave trains each characterised by its height  $H_i$ , period  $T_i$ , direction  $\alpha_i$  and frequency of occurrence,  $\phi_i$ . Each of the regular wave trains is then tracked across the coastal profile, which makes it possible to use the empirical non-linear wave height transformation inside the breaker line of this wave train and to take the integrated wave set-up caused by the combined wave trains into account. The directional spreading of the waves can be modelled by prescribing the distribution of wave directions for a series of wave trains, or by reducing the driving shear radiation stress of the wave trains according to the directional distribution of the wave energy. The results used here are based on the latter method using the cosine spreading function (Mitsuyasu et al. (1975) :

$$H(\theta) = \frac{2^{2s-1}}{\pi} \frac{\Gamma^2(s+1)}{\Gamma(2s+1)} \cos^2 s ((\theta - \theta_0)/2), \quad (3)$$

where  $\theta$  is the direction relative to the main direction  $\theta_0$ .

The reduction of the shear force component of the radiation stress for this distribution is shown in Fig. 2. The effect of irregular waves is illustrated in Fig. 3, showing a longshore velocity profile generated by regular waves, by unidirectional waves with a Rayleigh distribution of the incoming waves, and by waves with a directional spreading characterised by Eq. (3) with  $s = 20$  and  $s = 3$ , and regular height of the incoming waves.

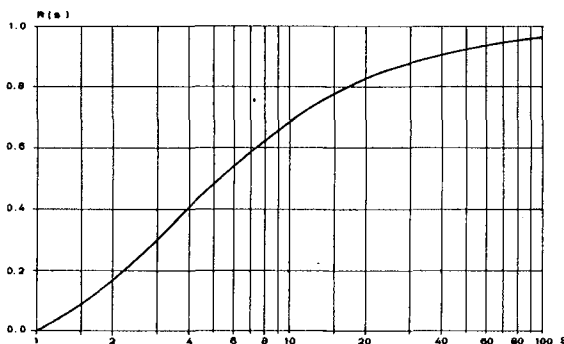


Fig. 2. The Reduction of the Longshore Shear Component of the Radiation Stress due to Directional Spreading.

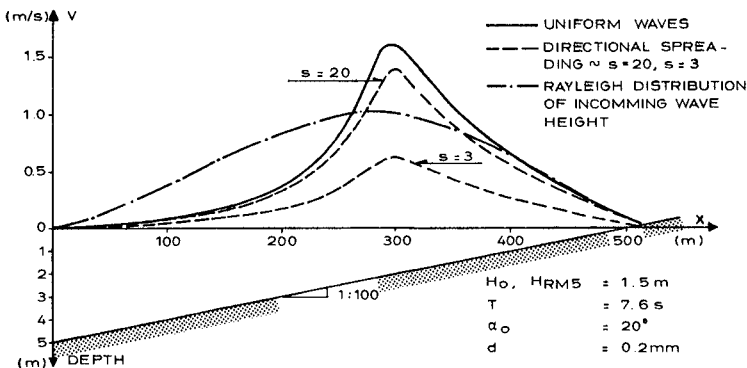


Fig. 3. Longshore Velocity Profiles.

The sediment transport rate is strongly influenced by the irregularity of the waves. The two most important effects are: A) The near bed orbital motion is irregular, which has to be taken into account when calculating the suspended sediment concentrations. B) In the surf zone only a fraction of the waves at a given point will be breaking/broken as there will be a fraction of the smaller waves which are breaking further inshore. The two effects are treated independently.

The irregular wave orbital motion has been analysed by using a time series of waves derived from a Pierson-Moskowitz spectrum. The nearbed wave orbital motion is calculated by a transfer function according to linear wave theory. The time series of the wave orbital velocity has been used in the model of Fredsøe et al. (1985) to calculate variation in time of the suspended sediment concentration and the sediment transport rate. The response of the mean current velocity profile to the irregular wave condition has not been analysed in detail, and two extreme situations have therefore been considered: 'full response' and 'no response'. By 'full response' it has been assumed that the mean current velocity profile outside the wave boundary layer adjusts immediately to the instantaneous wave conditions. In the case of 'no response' it has been assumed that the outer velocity and eddy viscosity profiles are determined from the mean bed shear stress integrated over the entire simulation period, and the outer velocity profile is thus kept constant.

Fig. 4 shows an example of a time series of water surface elevation and the suspended sediment transport rate.

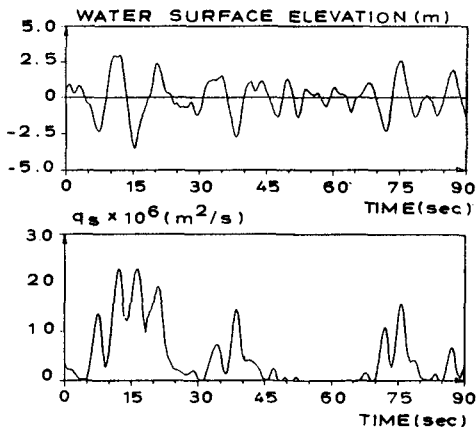


Fig. 4. Time Series of Surface Elevation, and Suspended Sediment Transport Rate,  $q_s$ , calculated for the following Parameters:

$H_{rms} = 3.5 \text{ m}$ ,  $T = 10 \text{ s}$ ,  $D = 10 \text{ m}$ ,  $V = 0.1 \text{ m/s}$ ,  
 $d = 0.22 \text{ mm}$ . 'Full Response'.

The purpose of these sediment transport calculations has been to determine the wave parameters which are best able to describe the time-averaged sediment transport under irregular waves.

In order to determine these wave parameters a series of numerical tests have been carried out. For all the tests,  $V$  was taken as  $0.1U_{b,rms}$  of the corresponding series, where  $U_{b,rms}$  is the root-mean-square of the orbital velocity amplitudes.

The value of  $q_s$  determined for each test was compared to that determined for a regular wave of height  $H$  and period  $T$ . From the analysis of the 16 combinations of  $H$  and  $T$  used for the sinusoidal motion it turns out that the best representation of the mean suspended sediment transport due to irregular waves over the whole range of values of  $U$  studied is given by the regular waves having  $H = H_{rms}$  and  $T = T_s$ , as shown by Fig. 5.

Fig. 5 also illustrates the influence of changing the eddy viscosity profile outside the wave boundary layer from 'full response' to 'no response'. In general, the difference is of order 10% or less.

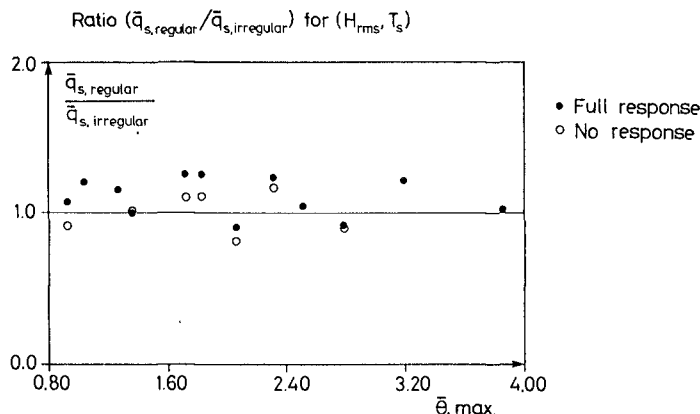


Fig. 5. Comparison between the Mean Suspended Sediment Transport due to Regular and Irregular Waves, and Illustration of the Influence of Current Response.

In the surf zone only a fraction of the waves is breaking due to the irregularity. The effect of breaking and broken waves is modelled according to Deigaard et al. (1986a) by describing the production, vertical spreading and decay of turbulence generated by the passage of the front of a spilling breaker or a broken wave. The input parameters, wave height  $H_b$  and period  $T_b$ , to this model are modified to reflect the conditions in the surf zone with irregular waves. First the wave period is increased to actual period of wave breaking, i.e. the non-broken waves are neglected, cf. Fig. 6.

$$T_b = \frac{\sum T_i \phi_i}{\sum \phi_{bi}} \quad (4)$$

where subscript 'bi' indicates that only breaking/broken waves are considered.

The representative wave height is determined from the energy dissipation, using a bore to characterise the dissipation in the passing wave fronts. The dissipation is thus proportional to the cube of wave height, giving:

$$H_b^3 = \frac{\sum H_{bi}^3 \phi_{bi}}{\sum \phi_{bi}} \quad (5)$$

This wave height and period is thus used in each location to characterise the production of turbulence by passing breaking or broken waves.

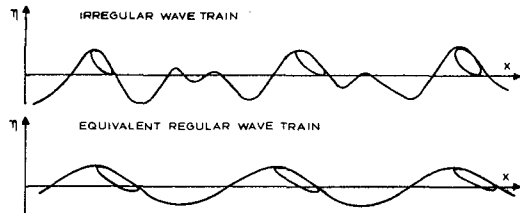


Fig. 6. Illustration of an Irregular Wave Train and the Equivalent Regular One.

Fig. 7 shows examples of the distribution of the transport in the coastal profile, calculated from regular and irregular waves. The main effect of including irregular waves is a much more smooth distribution of the transport and a reduction of the total transport by a factor of 0.3 in this particular case. The directional spreading of the waves  $s = 20$  and  $s = 3$  causes a reduction of the sediment transport in regular unidirectional waves by a factor 0.7 and 0.1, respectively.

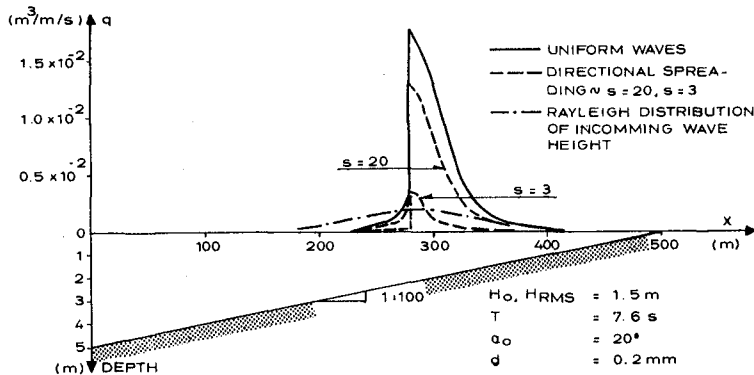


Fig. 7. Distributions of the Longshore Sediment Transport across a Plane Coast.

A comparison has been made between the calculated longshore sediment transport and the backfilling of a 1.600 m long trench (volume:  $200.000 \text{ m}^3$ ) dredged through a three-bar coastal profile at the Danish North Sea Coast, cf. Mangor et al. (1984). The backfilling during a storm in the spring of 1982 is considered with measured wave heights up to  $H_s = 4.75 \text{ m}$ . At this period the trench, width 90 m,

depth 10 m, was only dredged at the outer bar. The total backfilling of the trench in this period was measured to be 90.000 m<sup>3</sup> (solid) grain volume. Fig. 8 shows the distribution of the backfilling and the calculated distribution of the longshore transport on the outer bar during the storm. The wave heights have been assumed to follow the Rayleigh distribution. The calculations have been made for two directional spreadings, *s*, of which the smallest one is the most likely on that specific location.

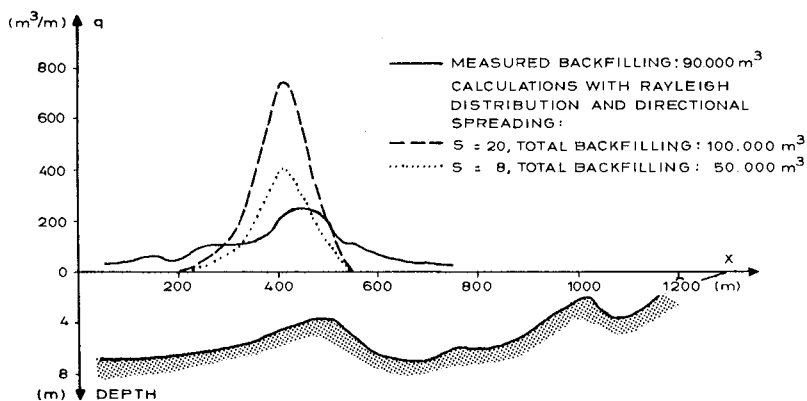


Fig. 8. Comparison between Measured Backfilling, cf. Mangor et al. (1984), and Calculated Backfilling.

#### WIND-DRIVEN AND COASTAL CURRENTS

In addition to radiation stress gradients, wind and coastal current can contribute to the forces driving the longshore current. The effect of wind shear stress and a coast parallel current has been included in the model. The wind shear stress is expressed through a friction factor (given the value:  $f_w = 0.005$ ) and the wind speed,  $U_{10}$  at 10 m elevation:

$$\tau_w = \frac{\rho_a}{2} f_w U_{10}^2 \quad (6)$$

$\rho_a$  is the density of air.  $\tau_w$  is resolved into a shore normal and a shore parallel component according to the angle  $\alpha$  between the wind direction and the shore normal direction. The shore normal component is included in the calculation of set-up and the shore parallel component is added to the driving forces of the littoral current.

The coastal current is assumed to be driven by a shore parallel gradient of the water surface,  $I$ , and the contribution to the driving force for the littoral current is  $\rho g D I$ , where  $D$  is the local water depth.

The resulting equation for the littoral current thus becomes:

$$\tau_b - \frac{d}{dx} (\rho E D \frac{dV}{dx}) = - \frac{ds_{xy}}{dx} + \tau_w \sin \alpha_w + \rho g D I \quad (7)$$

The effect of wind and current has been analysed for the basic conditions:  $H_s = 1.5$  m,  $T = 7.6$  s,  $d = 0.2$  mm, and a coastal slope of 1:100. Three wave directions are considered:  $\alpha_w = 10^\circ, 20^\circ$ , and  $45^\circ$ . Three wind speeds have been considered  $U_{10} = 5$  m/s, 10 m/s and 20 m/s, the wind is assumed to be parallel to the direction of wave propagation at deep water. Three coastal current velocities, measured at 5 m water depth, are analysed:  $V = -0.25$  m/s, 0.25 m/s, and 0.50 m/s.

The results are summarised in Fig. 9, showing the transport, normalised by the situation without wind or coastal current plotted against the total driving force normalised by the driving force due to waves alone. The driving force due to wind or water surface slope has been integrated over the area between the breaker line and the coastline, while the driving force due to the waves is the shear radiation stress,  $s_{xy}$ , at the breaker line. The driving forces due to waves, wind and water slope can easily be calculated, and generalised plots similar to Fig. 9 can then be used to estimate the relative importance of the different contributions. The difference between the effect of wind and current, revealed in Fig. 9, is due to the difference in distribution across the coastal profile; wind shear stress is constant while current-induced bed shear stress decreases with decreasing depth. For the same integrated force the coastal current will thus give a larger contribution near the breaker line where the sediment concentration and transport are highest.

#### RIP CURRENT

Along natural coasts bars, interrupted by rip channels, often show up as a result of a complex current and sediment transport pattern.

Rip currents can be generated as follows: The incoming waves break on the foreslope of the bar. When the waves pass the crest of the bar and enter the deeper waters of the trough, they cease breaking and are reformed as non-breaking waves, and shoaled and refracted once again until breaking occurs again on the inner beach.

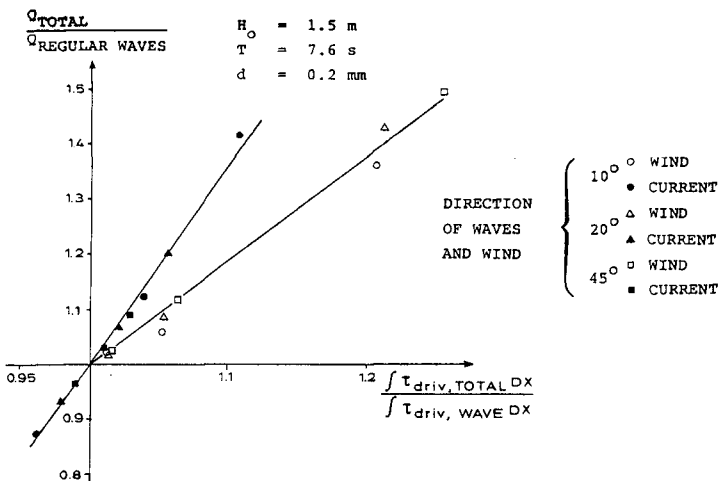


Fig. 9. The Sediment Transport including the Effect of Wind or Current normalised by the Transport due to Waves only versus the Total Driving Forces Normalised by Driving Forces due to Waves only.

The process of wave-breaking dissipates energy, producing a gradient in the components of the radiation stress tensor  $S$ . At the holes, the greater depths will cause that the waves are not breaking, but will instead continue propagation towards the shoreline. As a result of this, the wave set-up produced by the cross-shore component of the radiation stress  $S_{xx}$  will be small at the holes, and greater behind the bar.

This results in a net pressure gradient accelerating the water at the trough towards the holes. Afterwards this mass of water flows through the holes in the seaward direction in the form of rip-currents. The amount of water carried by the rips is compensated by the water transported over the crest of the bar. Under these conditions, a flow will exist at the trough behind the bar even for waves having an angle of incidence normal to the shoreline.

A mathematical model of flow in this situation has been developed. The model solves a simplified version of the equations describing the conservation of mass and momentum for time- and depth-averaged steady flow, see Zyserman and Fredsøe (1988).

Fig. 10 shows the flow field obtained using this model when the bar length was  $L = 180$  m, the width of the holes was  $Y_b = 50$  m, and the coastal profile was as shown on Fig.

10. The parameters of the incoming (uniform, unidirectional) waves were as follows:  $H_o = 1.2$  m,  $T = 7.5$  s,  $\alpha_o = 45^\circ$ . For comparison the corresponding longshore current velocity profile for a uniform coast is shown.

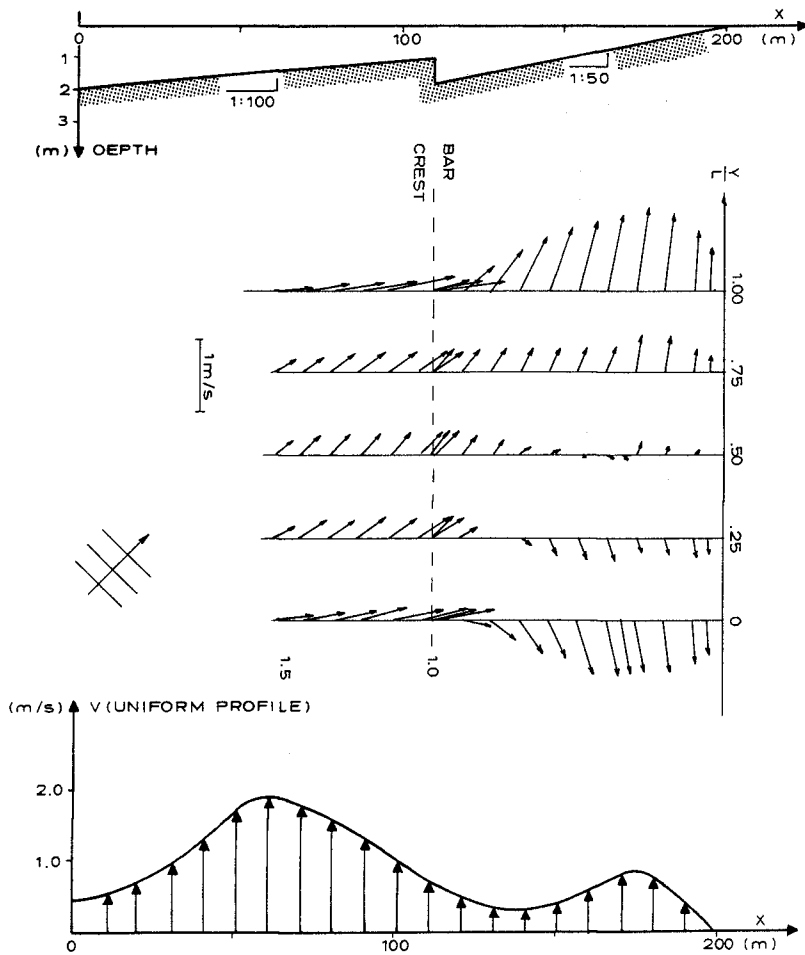


Fig. 10. Wave-Generated Currents on a Barred Coast with and without Rip Channels.

The following conclusions can be extracted from the results obtained for the wave-induced flow: a) The maximum velocity of the current on the bar is greatly reduced. The main cause for this is the cross-shore flow over the bar. The water carried in from offshore must continuously be accelerated up to the longshore velocity, which drains a considerable amount of longshore momentum. b) The flow reverses at some locations in the trough due to the pressure gradient which is opposite to the forcing term provided by the gradient of the shear component of the radiation stress tensor,  $S_{xy}$ . c) The velocity of the flow in the trough behind the bar crest becomes important, especially close to the holes.

Calculated current fields have been combined with the sediment transport model to describe the cross-shore variation of the longshore transport  $q_s$  as well as the total longshore transport  $Q_s$  for several transversal sections along the bar.

Due to the variability of the longshore current profile along the bar, the total transport varies from one section to another. In order to compare the sediment transport with that corresponding to the uniform situation, the average value of  $Q_s$  along the bar was calculated.

Fig. 11 shows the relation between the average longshore sediment transport when rip-currents are present  $\bar{Q}_s$  and the transport for the uniform situation  $Q_s$  as a function of the ratio between  $y_b$  and  $L$ , where  $y_b$  has been kept constant equal to 50 m. In these examples the characteristics of the shore and of the waves were chosen as for the situation, shown in Fig. 10.

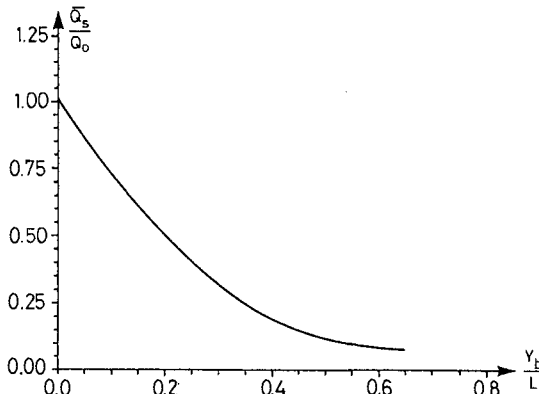


Fig. 11. Influence of Rip Currents on the Longshore Transport of Sediment. Coastal Profile and Wave conditions as Fig. 10.

It can be seen that the longshore sediment transport decreases for decreasing distance between rips, i.e. for shorter bars. This fact is easily explained by the reduction in the magnitude of the longshore current velocity when  $L$  decreases, due to an increased influence of the rip-currents.

#### CONCLUSION

A detailed description of littoral drift has been applied on a natural environment. It can be concluded that such a detailed model is rather sensitive to even small changes in the hydrodynamic description.

The following can be concluded from the test examples carried out with the extended littoral drift model including irregular waves, Fig. 7, coastal current and wind, Fig. 9, and the calculation of sediment transport along a barred coast with rip channels, Fig. 11:

- Both the irregularity of the waves and the presence of rip channels strongly reduce the total littoral drift compared to monochromatic waves and uniform conditions.
- The modifications of the littoral drift due to coastal current and wind action are less important.

The analysis rises a more general conclusion concerning the subject - modelling of littoral drift: Bearing in mind that all parameters in the models represent a physical phenomenon it must be concluded that the calculated littoral drift varies considerably by changing these parameters inside realistic ranges. The above means that modelling the littoral drift demands more information about the conditions (waves, coastal profiles etc.) than up till now has been established as basis for an investigation of littoral drift.

## REFERENCES

- Battjes, J.A. (1974) Computation of Set-up, Longshore Currents, Run up and Overtopping due to Wind-Generated Waves. Delft Technische Hogeschool.
- Deigaard, R., Fredsøe, J. and Hedegaard, I.B. (1986a) Suspended sediment in the surf zone. Journal of the Waterway, Port, Coastal and Ocean Engineering, ASCE, Vol. 112, No. 1, pp. 115-128.
- Deigaard, R., Fredsøe, J. and Hedegaard, I.B. (1986b) Mathematical model for littoral drift. Journal of the Waterway, Port, Coastal and Ocean Engineering, ASCE, Vol. 112, No. 3, pp. 351-369.
- Engelund, F. and Fredsøe, J. (1976) A sediment transport model for straight alluvial channels, Nordic Hydrology, 7, pp. 293-306.
- Fredsøe, J. (1984) The turbulent boundary layer in combined wave-current motion. Journal of Hydraulic Engineering, ASCE, Vol. 110, No. HY8, pp. 1103-1120.
- Fredsøe, J., Andersen, O.H. and Silberg, S. (1985) Distribution of suspended sediment in large waves. Journal of the Waterway, Port, Coastal and Ocean Engineering, ASCE, Vol. 111, No. 6, pp. 1041-1059.
- Mangor, K., Sørensen, T. and Navntoft, E. (1984) Shore approach at the Danish North Sea Coast, monitoring of sedimentation in a dredged trench. Proc. Coastal Engineering Conference, pp. 1818-1829.
- Mitsuyasu, H., Tasau, F., Suhara, T., Mizuno, S., Ohkusu, M., Honda, T. and Rikiishi, K. (1975) Observations of the directional spectrum of ocean waves using a clover leaf buoy. Journ. Phys. Oceanography, Vol. 5, pp. 750-760.
- Zyserman, J. and Fredsøe, J. (1988) The effect of rip-currents on the longshore sediment transport. Second International Symposium on Wave Research and Coastal Engineering, Hannover, F.R. of Germany.